Asian Journal of Chemistry; Vol. 36, No. 1 (2024), 125-134

ASIAN JOURNAL OF CHEMISTRY

https://doi.org/10.14233/ajchem.2024.30779

Benzofuran-Isoxazole Hybrids: Synthesis, Antimicrobial Activity and Dual Target Docking Studies

BHARGAVI POSINASETTY[1,2], RAJENDRA PRASAD YEJJELLA[3], KISHORE BANDARAPALLE[4], RAJASEKHAR KOMARLA KUMARACHARI[5,*], HARI VELURU[6] and CHILAMAKURU NARESH BABU[7]

[1]Department of Public Health, University of Southern Mississippi, MS-39406, USA
[2]Government Dental College and Research Institute, Bellary-583104, India
[3]Department of Pharmaceutical Chemistry, University College of Pharmaceutical Sciences, Andhra University, Visakhapatnam-530003, India
[4]Department of Pharmaceutics, Sri Padmavathi School of Pharmacy, Tiruchanur, Tirupati-517503, India
[5]Department of Pharmaceutical Chemistry, Sri Padmavathi School of Pharmacy, Tiruchanur, Tirupati-517503, India
[6]MB School of Pharmaceutical Sciences (Erstwhile Sree Vidyanikethan Colege of Pharmacy), Mohan Babu University, Sree Sainath Nagar, A. Rangampeta, Tirupati-517102, India
[7]Raghavendra Institute of Pharmaceutical Education and Research, Ananthapuramu-515721, India

*Corresponding author: Fax: +91 877 2237732; E-mail: komarla.research@gmail.com

Received: 8 October 2023; *Accepted*: 18 November 2023; *Published online*: 31 December 2023; AJC-21494

In this study, five novel heterocyclic molecular hybrids (**4a-e**) were synthesized by combining benzofuran and isoxazole motifs. These compounds were synthesized *via* a multistep process starting with 5-chlorosalicylaldehyde. The structures of the synthesized compounds were characterized by IR, ^{1}H NMR and mass spectrometry. Computational tools were employed to predict properties, including antitubercular and antibacterial traits, drug-likeness, bioactivity scores, toxicity and potential molecular targets. In addition to these predictions, *in vitro* bioactivities were assessed and conducted Schrödinger docking simulations to determine binding affinities to *Mycobacterium tuberculosis* enoyl-ACP reductase and *Escherichia coli* topoisomerase IV. Antitubercular efficacy was determined *via* the MABA method, while antibacterial effectiveness was tested against both Gram-positive and Gram-negative bacteria. The obtained results highlighted the promise of these benzofuranyl-isoxazole hybrids, making them strong contenders for further lead optimization, with the goal of developing more potent and safer pharmaceutical agents.

Keywords: Benzofuran-isoxazole hybrids, *In vitro* antitubercular activity, Antibacterial activity, Dual target docking.

INTRODUCTION

Heterocyclic molecular hybrids are the chemical compounds formed by combining two or more heterocyclic rings. These hybrid compounds find multifaceted applications across various domains, particularly in medicinal chemistry, where they are strategically designed to enhance drug properties [1-3]. Their diverse structures and properties make them invaluable for constructing innovative compounds tailored for specific functions, allowing them to span a wide spectrum of biological activities.

Benzofurans and isoxazoles are the two essential classes of heterocyclic compounds with distinct structures and properties [4]. Benzofurans consist of a fused benzene ring and an oxygen atom in a five-membered ring. This structural motif has garnered attention due to its potential as a pharmacophore in drug design [5]. They are known for their antitubercular [6], antibacterial [7], antimicrobial [8], antifungal [9], anti-inflammatory [10], anticancer [11] and neuroprotective properties [12], making them promising candidates for the development of novel pharmaceutical agents.

Similarly, isoxazoles are also another class of heterocyclic compounds featuring a five-membered ring containing both nitrogen and oxygen atoms. Their structural features make them essential building blocks in organic synthesis, contributing to the creation of bioactive compounds. Isoxazoles are also recognized for their antimicrobial [13,14], anticancer [15,16], anticholinesterase [17] and diuretic properties [18].

The amalgamation of benzofurans and isoxazoles into hybrid compounds presents an exciting avenue in the field of

medicinal chemistry and drug discovery [19]. The significance of these hybrids lies in the potential synergy of their individual properties. By fusing benzofuran and isoxazole moieties, can design molecules that capitalize on the advantageous characteristics of both structural elements. This can result in compounds with enhanced bioactivity, improved pharmacokinetics, and a broader range of potential therapeutic applications [20,21].

Motivated by the information on benzofuran and isoxazole derivatives, we have synthesized benzofuran-isoxazole hybrids targeting potential pharmacophores. Given the ongoing global challenges related to infectious diseases and antibiotic resistance, the antimicrobial properties of these hybrids are of paramount interest [22-25]. Through evaluating the antimicrobial efficacy of these compounds against a range of pathogens, we aim to identify potential candidates for further development as antibiotics or antimicrobial agents. To make predictions about the properties of these molecules, the computational tools like PASS, Molinspiration, Osiris and Swiss ADME were employed. These predictions encompassed factors such as antitubercular and antibacterial traits, drug-likeness, bioactivity scores, toxicity and potential molecular targets.

Moreover, the inclusion of dual target docking studies adds a computational dimension to the investigation [26]. This involves assessing the binding affinity of the synthesized benzofuran-isoxazole hybrids to two specific molecular targets: one associated with mycobacterial pathogens and another relevant to potential antibacterial therapeutic interventions. These studies offer insights into the potential modes of action and molecular interactions underlying the observed antimicrobial activity, providing a deeper understanding of the compounds' mechanisms. This research has the potential to yield valuable insights into the development of novel antimicrobial agents, contributing to the ongoing efforts to combat infectious diseases and antibiotic resistance.

EXPERIMENTAL

All chemicals employed in this research were meticulously sourced from reputable suppliers, including Sigma Aldrich Co. (St. Louis, USA), Merck (Whitehouse Station, USA), Qualigens Fine Chemicals (Mumbai, India), Loba Chemie Pvt. Ltd. (Mumbai, India), and Himedia Laboratories Pvt. Ltd. (Mumbai, India).

To determine the melting points of the synthesized compounds, a digital melting point apparatus with open capillary tubes was utilized. The reported values are presented without correction. The evaluation of compound purity was conducted through thin-layer chromatography, making use of pre-coated silica gel strips and a solvent system comprising a 2:1 ratio of hexane to ethyl acetate. Visualization of the chromatographic spots was achieved using an ultraviolet chamber.

Infrared spectra (expressed in ν/cm) were recorded using a Shimadzu FT-IR 4000 instrument equipped with KBr disks. The CHNO elemental analysis was executed using the Perkin-Elmer Series II 2400 CHNS/O Elemental Analyzer. Mass spectra were obtained *via* a JEOL GC mate II GC-Mass spectrometer, which operated at 70 eV and employed the direct insertion probe method. For the collection of NMR spectra, a Bruker AVIII-500 MHz FT NMR spectrometer was utilized, with TMS serving as the internal standard and DMSO as solvent.

Synthetic procedure: Scheme-I illustrates the synthesis of all the compounds, starting with 5-chloro-salicylaldehyde (**1**) synthon. Initially, this 5-chlorosalicyl-aldehyde underwent a cyclization process, resulting in the formation of the pivotal synthon, 5-chloro-2- acetylbenzofuran (**2**). Next, the acetyl group was converted to prop-2-en-1-one through a Claisen-Schmidt condensation reaction with various aromatic aldehydes. These sequential chemical transformations culminated in the synthesis of pivotal intermediates known as 1-(5-chloro-1-benzofuran-2-yl)-3-substituted phenyl prop-2-en-1-ones (chalcones **3a-e**).

The next phase of the synthesis involved the reaction of these chalcones (**3a-e**) with hydroxylamine, yielding the final compounds, 3-(5-chloro-1-benzofuran-2-yl)-5-(substituted phenyl)-4,5-dihydroisoxazoles (**4a-e**). This synthetic pathway allows for the controlled construction of the target molecular hybrids through a series of well-defined chemical transformations, ensuring the formation of the desired benzofuran-isoxazole hybrid compounds.

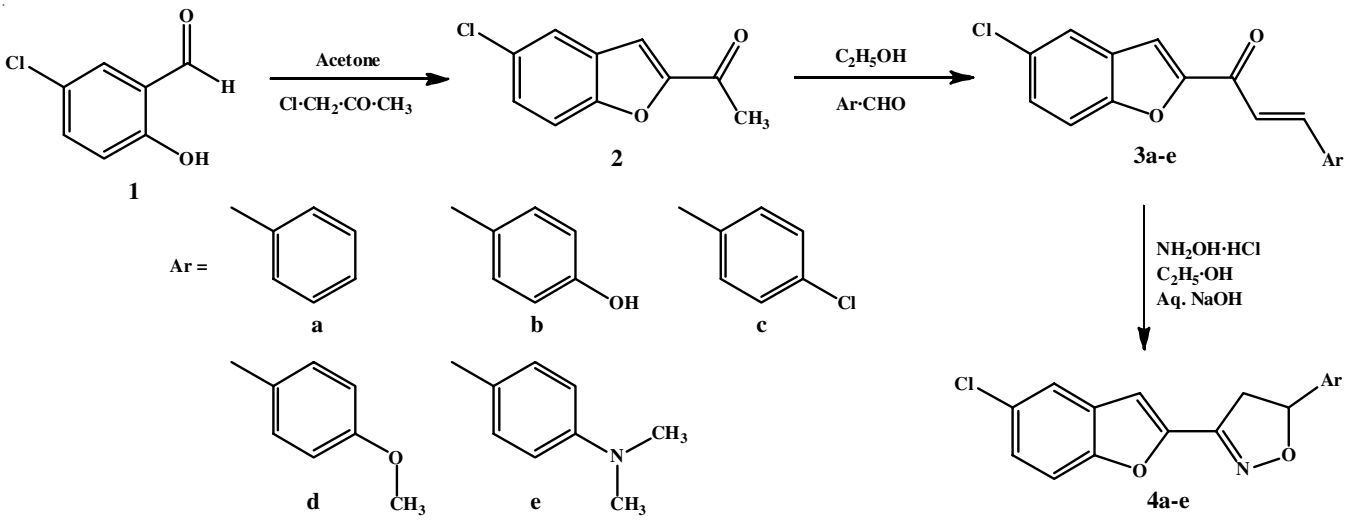

Scheme-I: General synthesis of 3-(5-chloro-1-benzofuran-2-yl)-5-(substitutedphenyl)-4, 5-dihydro isoxazoles (**4a-e**)

Synthesis of 5-chloro-2-acetylbenzofuran (2): A mixture containing 5-chlorosalicylaldehyde (**1**), chloroacetone (4.63 g, 0.05 mol), and anhydrous K_2CO_3 (15 g) was gently refluxed in dry acetone (50 mL) for 12 h. After the completion of the reaction, the reaction product was filtered and the filtrate was subjected to solvent removal under reduced pressure. This process yielded 5-chloro-2-acetylbenzofuran (**2**) as a light brownish solid. The obtained product was further purified by recrystallized from ethanol. Yield: 75 %; m.p.: 83-85 ºC. IR (KBr, ν_{max}, cm^{-1}): 1666 (C=O), 1461 (C=C) and 790 (CCl), MS (*m/z*, %): 194 (M+) and 196 (M+2+), ^{1}H NMR (δ ppm): 7.2-7.8 (4Ar-H), 2.6 (3H, s, CH_3).

General synthesis of 1-(5-chloro-1-benzofuran-2-yl)-3-(substitutedphenyl)-prop-2-en-1-ones (3a-e): A mixture consisting of 5-chloro-2-acetylbenzofuran (**2**) (1.94 g, 0.01 mol) and various substituted aromatic aldehydes (0.01 mol), in 50 mL of ethanol was cooled to a temperature between 5-10 ºC. Aqueous NaOH (70%, 5 mL) was then added dropwise with constant stirring. The reaction mixture was further stirred for a duration of 2 h and left overnight. Subsequently, it was neutralized with conc. HCl. The solid product that separated out was collected and further purified by crystallization from ethanol. The purity of all the synthesized compounds was confirmed by thin-layer chromatography (TLC) using a mobile phase consisting of a mixture of hexane and ethyl acetate.

General synthesis of 3-(5-chloro-1-benzofuran-2-yl)-5-(substituted phenyl)-4,5-dihydroisoxazoles (4a-e): A mixture of 1-(5-chloro-1-benzofuran-2-yl)-3-(substituted phenyl)prop-2-en-1-one (**3a-e**, 0.01 mol) and hydroxylamine hydrochloride (0.01 mol) in anhydrous ethanol (50 mL) was prepared. To this mixture, 10% aqueous NaOH (6 mL) was added and the reaction was refluxed for 5 h. The reaction mixture was then poured into ice-cold water and the resulting product was filtered, washed with water and recrystallized using ethanol as solvent. The purity of the compound was verified *via* TLC using a hexane and ethyl acetate mixture as the mobile phase. By adopting the above synthetic procedures, compounds **3a-e** and **4a-e** were also synthesized.

3-(5-Chloro-1-benzofuran-2-yl)-5-phenyl-4,5-dihydro-1,2-oxazole (4a): Yield: 70%: m.p.: 168-171 ºC; FT-IR (KBr, ν_{max}, cm^{-1}): 1568 (C=N), 1448 (C=C), 800 (C-Cl); ^{1}H NMR (DMSO-d_6, δ ppm): 3.01-3.20 (2H, 3.08 (d), 3.13 (d), 6.14 (1H, d), 7.24-7.50 (6H, 7.30 (d), 7.38 (t), 7.43 (d), 7.42 (d), 7.52-7.80 (3H, 7.57 (d), 7.68 (d), 7.75 (d); MS (*m/z*, %): 297.72 (M+). Anal. calcd. (found) % for $C_{17}H_{12}NO_2Cl$: C, 68.58 (68.64); H, 4.06 (4.10); N, 4.70 (4.76): O, 10.75 (10.78).

4-[3-(5-chloro-1-benzofuran-2-yl)-4,5-dihydro-1,2-oxazol-5-yl]phenol (4b): Yield: 65%: m.p.: 179-181 ºC; FT-IR (KBr, ν_{max}, cm^{-1}): 3747 (OH), 1561 (C=N), 1442 (C=C), 804 (C-Cl); ^{1}H NMR (DMSO-d_6, δ ppm): 3.00-3.17 (2H, 3.08 (d), 3.09 (d), 6.04 (1H, d), 6.69 (2H, d), 7.24-7.43 (3H, 7.30 (d), 7.37 (d), 7.52-7.80 (3H, 7.57 (d), 7.68 (d), 7.75 (d), 9.8 (1H,d); MS (*m/z*, %): 313.74 (M+). Anal. calcd. (found) % for $C_{17}H_{12}NO_3Cl$: C, 65.08 (65.12); H, 3.86 (3.91); N, 4.46 (4.42): O, 15.30 (15.36).

3-(5-Chloro-1-benzofuran-2-yl)-5-(4-chlorophenyl)-4,5-dihydro-1,2-oxazole (4c): Yield: 68%: m.p.: 204-207 ºC; FT-IR (KBr, ν_{max}, cm^{-1}): 1560 (C=N), 1458 (C=C), 798 (C-Cl); ^{1}H NMR (DMSO-d_6, δ ppm): 3.02-3.20 (2H, 3.10 (d), 3.13 (d), 6.16 (1H, d), 7.30 (1H, d), 7.40-7.80 (7H, 7.46 (d), 7.56 (d), 7.57 (d), 7.68 (d), 7.75 (d); MS (*m/z*, %): 332.18 (M+). Anal. calcd. (found) % for $C_{17}H_{11}NO_2Cl_2$: C, 61.47 (61.52); H, 3.34 (3.37); N, 4.22 (4.26): O, 9.63 (9.67).

3-(5-Chloro-1-benzofuran-2-yl)-5-(4-methoxyphenyl)-4,5-dihydro-1,2-oxazole (4d): Yield: 72%: m.p.: 193-196 ºC; FT-IR (KBr, ν_{max}, cm^{-1}): 1548 (C=N), 1444 (C=C), 1124(C-O), 804 (C-Cl); ^{1}H NMR (DMSO-d_6, δ ppm): 2.98-3.15 (2H, 3.06 (d), 3.08 (d), 3.75 (3H, s), 6.04 (1H, d), 6.89 (2H, d), 7.24-7.43 (3H, 7.30 (d), 7.36 (d), 7.52-7.80 (3H, 7.57 (d), 7.68 (d), 7.75 (d); MS (*m/z*, %): 327.76 (M+). Anal. calcd. (found) % for $C_{18}H_{14}NO_3Cl$: C, 65.96 (65.91); H, 4.31 (4.34); N, 10.82 (10.84): O, 14.64 (14.67).

4-[3-(5-Chloro-1-benzofuran-2-yl)-4,5-dihydro-1,2-oxazol-5-yl]-N,N-dimethylaniline (4e): Yield: 60%: m.p.: 214-218 ºC; FT-IR (KBr, ν_{max}, cm^{-1}): 1566 (C=N), 1447 (C=C), 1248 (C-N), 783 (C-Cl); ^{1}H NMR (DMSO-d_6, δ ppm): 2.74 (6H, s), 2.97-3.17 (2H, 3.05 (d), 3.09 (d), 6.00 (1H, d), 6.66 (2H, d), 7.12-7.36 (3H, 7.18 (d), 7.30 (d), 7.52-7.80 (3H, 7.57 (d), 7.68 (d), 7.75 (d); MS (*m/z*, %): 340.80 (M+). Anal. calcd. (found) % for $C_{19}H_{17}N_2O_2Cl$: C, 66.96 (66.92); H, 5.03 (5.06); N, 8.22 (8.25): O, 9.39 (9.43).

Prediction of biological activity: The title compounds underwent pharmacological activity prediction using the online tool PASS. This predictive system compares the structures of the novel compounds with well-established biologically active substances to identify potential pharmacological properties, which can later be confirmed through experimental studies. PASS's advantage lies in its vast database, featuring thousands of substances from the training set, enabling a more objective estimation of potential biological activities. Furthermore, it requires only the structural formula or SMILES of the chemical compound, making it applicable at an early stage of investigation [27]. Following the submission of the title compounds' structures to the PASS online program, various potential mechanisms of action and biological activities were predicted. Notably, the compounds exhibited a higher likelihood of demonstrating activity as antitubercular and antibacterial agents.

Molinspiration: Molinspiration is a valuable resource for the online chemistry community, offering free online services for predicting bioactivity scores related to crucial drug targets. These targets encompass a wide range, from G protein-coupled receptor (GPCR) ligands to kinase inhibitors, ion channel modulators, enzymes, and nuclear receptors. Molinspiration's user-friendly and easily accessible platform plays a pivotal role in supporting the research endeavors of the online chemistry community, simplifying the exploration of molecular properties and bioactivity predictions for a diverse array of chemical compounds [28].

Osiris property explorer: The Osiris property explorer plays a crucial role within Actelion's in-house substance registration system. It enables users to draw chemical structures and upon validation, it performs real-time calculations of various properties relevant to drug development. The prediction results are presented with assigned values and colour codes for straightforward interpretation. Properties associated with a higher risk

of undesired effects, such as mutagenicity, are prominently highlighted in red, drawing attention to potential concerns. Conversely, properties indicative of drug-like behaviour are depicted in green, signaling promising characteristics for drug development. This colour-coded presentation significantly aids researchers in swiftly identifying compounds with desirable attributes and potential issues, streamlining the drug discovery and development process [29].

Swiss ADME: The Swiss ADME online platform's prediction tools were employed to evaluate a range of characteristics, including physico-chemical properties, lipophilicity, water solubility, pharmacokinetics, druglikeness, molecular target, and medicinal chemistry parameters. To estimate the drug-likeness of the compounds, *in silico* absorption, distribution, metabolism, excretion and toxicity (ADMET) predictions were conducted for the synthesized compounds **4a-e** using the Swiss-ADME software [30].

Dual target docking studies

Preparation of target molecules: To prepare the target molecules, a dual target docking study was conducted using the GLIDE docking program (Schrödinger 2020-1) [31]. The synthesized compounds (**4a-e**) underwent docking within the active sites of two crystal structures: *Mycobacterium tuberculosis* enoyl-ACP reductase (PDB code: 2PR2) and *Escherichia coli* Topoisomerase IV ParE 24kDa subunit (PDB code: 1S14).

The quality of the target protein structures was meticulously assessed using various tools, including ERRAT, Verify 3D and the structural analysis and verification server [32-34]. These analyses verified the acceptability and high quality of all protein models. Furthermore, a comprehensive analysis of the Ramachandran plot was performed using RAMPAGE to evaluate dihedral angles and permissible conformations [35].

Preparation of ligand molecules: In the process of preparing ligand molecules, the 2D chemical structures of compounds **4a-e** were initially drawn using Chem Draw Ultra Version 8.0.3 [36] and saved in binary format. These structures were then converted into the sdf format using the Open Babel GUI version 2.4.1, which is a versatile virtual screening tool designed for Windows [37,38]. Subsequently, a meticulous energy minimization was conducted using the OPLS3e force field with Ligprep. This process involved careful considerations, including ionization at a target pH of 7.0 ± 2.0, desalting and the preservation of specified chiralities [39]. To enable a comparative evaluation of binding affinities, ATP was used as the reference ligand in the docking experiments. The results were comprehensively assessed by scrutinizing binding interactions and docking scores obtained from GLIDE_SP ligand docking.

Antitubercular activity: The synthesized derivatives, specifically 3-(5-chloro-1-benzofuran-2-yl)-5-(substituted phenyl)-4,5-dihydro isoxazoles (**4a-e**) were subjected to screening for their antitubercular activity using the microplate Alamar blue assay method (MABA). Each of the synthesized compounds was tested against the *M. tuberculosis* H37 RV strain, with isonicotinic acid hydrazide (INH) used as the standard drug for comparison. For assay setup, 200 µL of sterile deionized water was introduced into the outermost wells of a sterile 96-well plate to prevent medium evaporation during incubation. Following this, 100 µL of Middlebrook 7H9 (MB 7H9) broth was carefully dispensed into the wells and the synthesized compounds were serially diluted directly on the plate. The antitubercular activity of these compounds was assessed at final drug concentrations of 0.2, 0.4, 0.8, 1.6, 3.125, 6.25, 12.5, 25, 50 and 100 µg/mL. The plates were covered, sealed with parafilm and then incubated at 37 ºC for 5 days. After the incubation period, 25 µL of a freshly prepared 1:1 mixture of Alamar blue reagent and 10% Tween-80 was added to each well. The plates were further incubated for an additional 24 h. The interpretation of the results was based on the color change observed in the wells: a blue color indicated no bacterial growth, while a pink color signified bacterial growth [40].

Antibacterial activity: The antibacterial activity of the synthesized compounds (**4a-e**) was evaluated using the agar cup plate method. Specifically, these compounds were tested against a range of bacteria, including Gram-negative organisms such as *Escherichia coli* and *Pseudomonas aeruginosa* as well as Gram-positive organisms, including *Staphylococcus epidermatitis* and *Bacillus subtilis*. The minimum inhibitory concentration (MIC) method was utilized for assessment with ciprofloxacin employed as a reference standard for result comparison.

During the procedure, the brain heart infusion agar was brought to room temperature. Colonies were then transferred to the plates and their turbidity was visually adjusted using broth to match the turbidity of a 0.5 McFarland turbidity standard that had been vortexed. To achieve uniform distribution, the entire surface of the agar plate was swabbed three times, with the plates rotated approximately 60º between each streaking. Following this step, the inoculated plate was allowed to stand for at least 5 min before the disks were applied. A 5 mm hollow tube was heated and pressed onto the inoculated agar plate, creating five wells in the plate, which were then promptly removed. Subsequently, 75, 50, 25, 10, and 5 µL of the synthesized compounds were added into the respective wells on each plate. The plates were then incubated within 15 min of compound application and were placed in an incubator at 37 ºC for 24 h. The diameter of the inhibition zone was measured to the nearest whole millimeter using a measuring device. The MIC procedure involved repeating the serial dilution up to a 10^{-9} dilution for each synthesized compound [41,42].

RESULTS AND DISCUSSION

Traditionally, chalcones have been synthesized *via* the Claisen-Schmidt reaction, which entailed stirring a ketone and aldehyde in an organic solvent, often with the assistance of an acid or base catalyst. The reaction of chalcones with hydroxylamine or a derivative of hydroxylamine results in the cyclization of chalcone molecule, leading to the formation of an isoxazole ring. In this study, we subjected the crucial intermediates, namely 1-(5-chloro-1-benzofuran-2-yl)-3-substituted phenyl prop-2-en-1-ones (**3a-e**) to a reaction with hydroxylamine to yield target compounds (**4a-e**). The purity of all the synthesized compounds (**2**, **3a-e** and **4a-e**) was confirmed using thin-layer chromatography (TLC), with a mobile phase consisting of a mixture of hexane and ethyl acetate. Their identity was further substan-

tiated by displaying a single spot on TLC, well-defined melting points, and characteristic spectral features.

In the infrared spectra of the synthesized compounds (**4a-e**), a distinct band around 1560 cm^{-1} was evident, confirming the presence of a C=N bond within the dihydroisoxazole ring, signifying the formation of the target compounds. In the ^1H NMR spectra of these compounds, signals for aromatic protons resonated within the range of 7.1 to 8.0 ppm, while signals for the characteristic dihydroisoxazole $–CH_2$ groups were observed around 3.0 ppm. Notably, compound **4b** exhibited a proton singlet at 9.8 ppm, corresponding to the proton of the hydroxy group located at the *para*-position of phenyl ring attached to the 5th position of isoxazole system. Mass spectrometry analysis further validated the presence of the expected molecular ion peak (M+) fragments for the synthesized compounds.

***In silico* profiling:** Table-1 presents the PASS-predicted biological activity profiles based on an extensive training dataset of 60,000 biologically active compounds across 4,500 distinct activities. Calculated probabilities (Pa and Pi) indicate specific activity likelihood. Initially, all the compounds were projected to exhibit antibacterial and antitubercular activities with Pa values below 0.5. However, the experimental assessments contradicted these predictions, revealing significant antibacterial and antitubercular activities, challenging the PASS's forecasts. In summary, PASS predicts promising pharmacological potential for these compounds, especially in antibacterial and antitubercular contexts. Subsequent experiments can validate these predictions, exploring their potential as novel pharmacologically active substances.

Molinspiration was utilized to predict the bioactivity scores for each of the synthesized compounds as depicted in Fig. 1. Compounds **4b** and **4e** emerged as standout performers among the synthesized compounds, displaying remarkable bioactivity values. These findings highlight the potential of these compounds as GPCR ligands, kinase inhibitors and enzyme inhibitors. Table-2 outlines the predicted toxicological properties and drug scores *via* the Osiris property explorer. Notably, all the five synthesized compounds were anticipated to have a favorable safety profile with no toxicity concerns and favorable drug scores. Regrettably, compound **4e** showed some tumorigenic potential, aligning with INH, a standard *in vitro* drug. Assessing drug-likeness considered various molecular properties and structural features, revealing the resemblance of the synthesized compounds to established drugs. The drug score, a condensed metric combining drug-likeness, cLogP, logS, molecular weight and toxicity risks, helps in evaluating the potential of compound for drug qualification. Except for compounds **4d** and **4e**, all

TABLE-1
PREDICTED BIOLOGICAL ACTIVITY SPECTRUM OF SYNTHESIZED COMPOUNDS (**4a-e**)

Compound	Pa	Pi	Activity
4a	0.506	0.023	Antiviral (Rhinovirus)
	0.300	0.60	Antibacterial
	0.218	0.126	Antifungal
	0.047	0.025	Enoyl-[acyl-carrier-protein] reductase (NADH) inhibitor
4b	0.489	0.028	Antiviral (Rhinovirus)
	0.345	0.045	Antibacterial
	0.274	0.093	Antifungal
	0.058	0.012	Enoyl-[acyl-carrier-protein] reductase (NADH) inhibitor
4c	0.512	0.02	Antiviral (Rhinovirus)
	0.314	0.055	Antibacterial
	0.222	0.123	Antifungal
	0.048	0.025	Enoyl-[acyl-carrier-protein] reductase (NADH) inhibitor
4d	0.433	0.053	Antiviral (Rhinovirus)
	0.270	0.072	Antibacterial
	0.204	0.134	Antifungal
	0.041	0.040	Enoyl-[acyl-carrier-protein] reductase (NADH) inhibitor
4e	0.441	0.055	Antiviral (Rhinovirus)
	0.280	0.068	Antibacterial
	0,197	0,108	Antifungal
	0,041	0,041	Enoyl-[acyl-carrier-protein] reductase (NADH) inhibitor
Isoniazid	0.810	0.003	Antituberculosic
	0.798	0.004	Antimycobacterial
	0.371	0.038	Antibacterial
	0.226	0.042	*trans*-2-Enoyl-CoA reductase (NAD+) inhibitor
Ciprofloxacin	0.639	0.008	Antimycobacterial
	0.588	0.009	Antibacterial
	0.452	0.019	Antituberculosic
	0.304	0.086	Antiviral (Adenovirus)

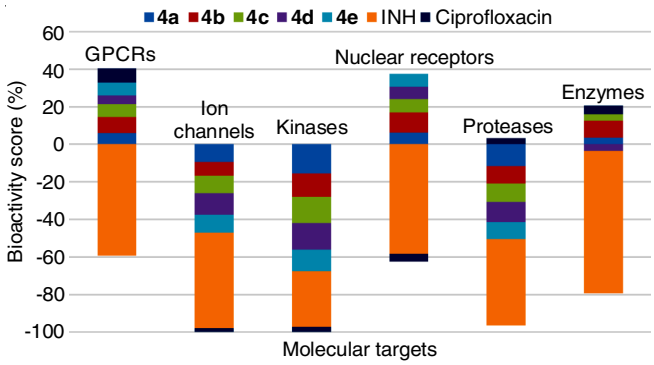

Fig. 1. Calculation of bioactivity scores using Molinspiration

TABLE-2
PREDICTIVE TOXICITY PROPERTIES USING OSIRIS MOLECULAR PROPERTY EXPLORER

Compound	Drug likeness	Drug score	Mutagenicity	Tumorigenicity	Irritant	Reproductive toxicity
4a	4.07	0.69	No	No	No	No
4b	4.05	0.72	No	No	No	No
4c	5.83	0.61	No	No	No	No
4d	2.37	0.66	No	No	No	No
4e	2.94	0.40	No	YES	No	No
Isoniazid	-5.06	0.06	YES	YES	YES	YES
Ciprofloxacin	2.07	0.89	No	No	No	No

other compounds scored well in their suitability for drug qualification.

Swiss ADMET predicted the physico-chemical, pharmacokinetic and medicinal chemistry properties. All the synthesized compounds adhered to Lipinski's rule, meeting criteria for drug-likeness with parameters like molecular weight, Clog P (lipophilicity), hydrogen bond donors and acceptors counts within limits. Table-3 shows that all compounds demonstrated high gastrointestinal absorption, blood-brain barrier permeability, and no skin permeation or pan assay interference structural alerts (PAINS). No compounds were predicted as P-glycoprotein substrates, validated with support vector machine (SVM) model. Using 1024 fragmental contributions (FP2), compounds **4a-e** were predicted to be easily synthesized, aligning well with observed yields.

Dual target docking studies: The quality of the 3D models for the target molecules was assessed using Ramachandran plot calculations *via* RAMPAGE. For 2PR2, 89.8% of residues were in the favoured region, 8.9% in the allowed region and 0.9% in the outlier region. For 1S14, these values were 94.6, 5.4 and 0%, respectively. These percentages, approaching 100%, indicate excellent model quality, affirming the high quality of the predicted models (Fig. 2). Additionally, the models underwent validation using other servers such as ERRAT and Verify 3D. ERRAT analysis yielded overall quality factors of 94.21% for 2PR2 and 95.83% for 1S14, both exceeding the 95% rejection limit and confirming the quality of the target protein models. Verify 3D analysis showed that all amino acids in 2PR2 received non-negative scores, while a few residues in 1S14 had marginally negative scores. Moreover, 99.25% of amino acid residues in 2PR2 and 46.43% in 1S14 exhibited 3D-1D scores greater than or equal to 0.2, indicating a structurally acceptable environment (Fig. 3).

Docking scores for each ligand against both target proteins were predicted using glide, a well-established Schrödinger docking software. Figs. 4 and 5 illustrate the docking of compounds **4a-e** with the two target protein models. In each docking process, ten binding poses were generated, and the pose with the highest docking score was selected. Among all the synthesized compounds, **4b** exhibited the highest docking score (-5.086 1S14). All compounds displayed promising docking scores comparable to their respective standards.

A summary of the interactions between the synthesized compounds (**4a-e**) and the amino acid residues of target proteins 2PR2 and 1S14 is presented in Tables 4 and 5. With the exception of compounds **4a**, **4c** and **4e**, all the synthesized compounds displayed both hydrogen bond and hydrophobic interactions with 2PR2. Furthermore, compounds **4a**, **4b** and **4d** exhibited hydrophobic interactions similar to the standard drug INH, albeit at different interaction sites. However, except compound **4b**, rest of the compounds achieved docking scores close to the standard score, indicating nearly equivalent binding affinity.

TABLE-3
PREDICTION OF PHARMACOKINETIC AND MEDICINAL CHEMISTRY PROPERTIES USING SWISS ADME

Compound	GIA[a]	BBBP[b]	P-gpS[c]	log Kp (cm/s)[d]	BAS[e]	PAINS alert	SA[f]
4a	High	Yes	No	-4.79	0.55	0	3.81
4b	High	Yes	No	-5.15	0.55	0	3.76
4c	High	Yes	No	-4.56	0.55	0	3.81
4d	High	Yes	No	-5.00	0.55	0	3.81
4e	High	Yes	No	-4.97	0.55	0	3.95
Isoniazid	High	No	No	-7.63	0.55	0	1.23
Ciprofloxacin	High	No	Yes	-8.53	0.55	0	3.22

a = Gastrointestinal absorption, b = Blood brain barrier permeant, c = P-gp substrate, d = Skin permeant, e = Bioavailability score and f = Synthetic accessibility

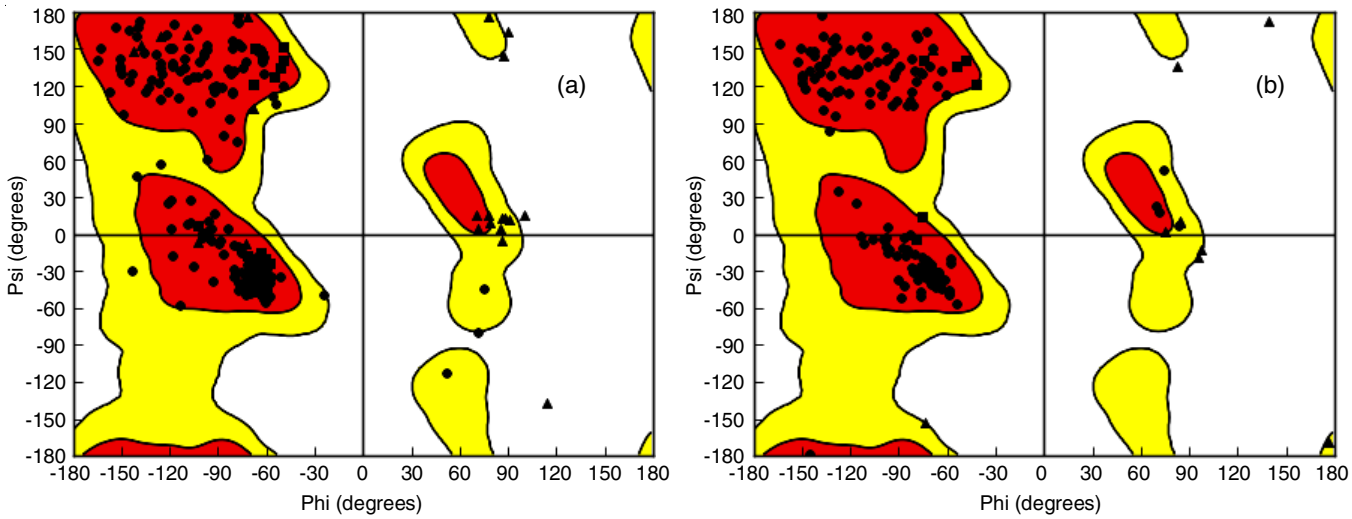

Fig. 2. Ramachandran plots generated *via* RAMPAGE for (a) 2PR2 and (b) 1S14. Residues in favoured (red), allowed (yellow) and outlier regions (white)

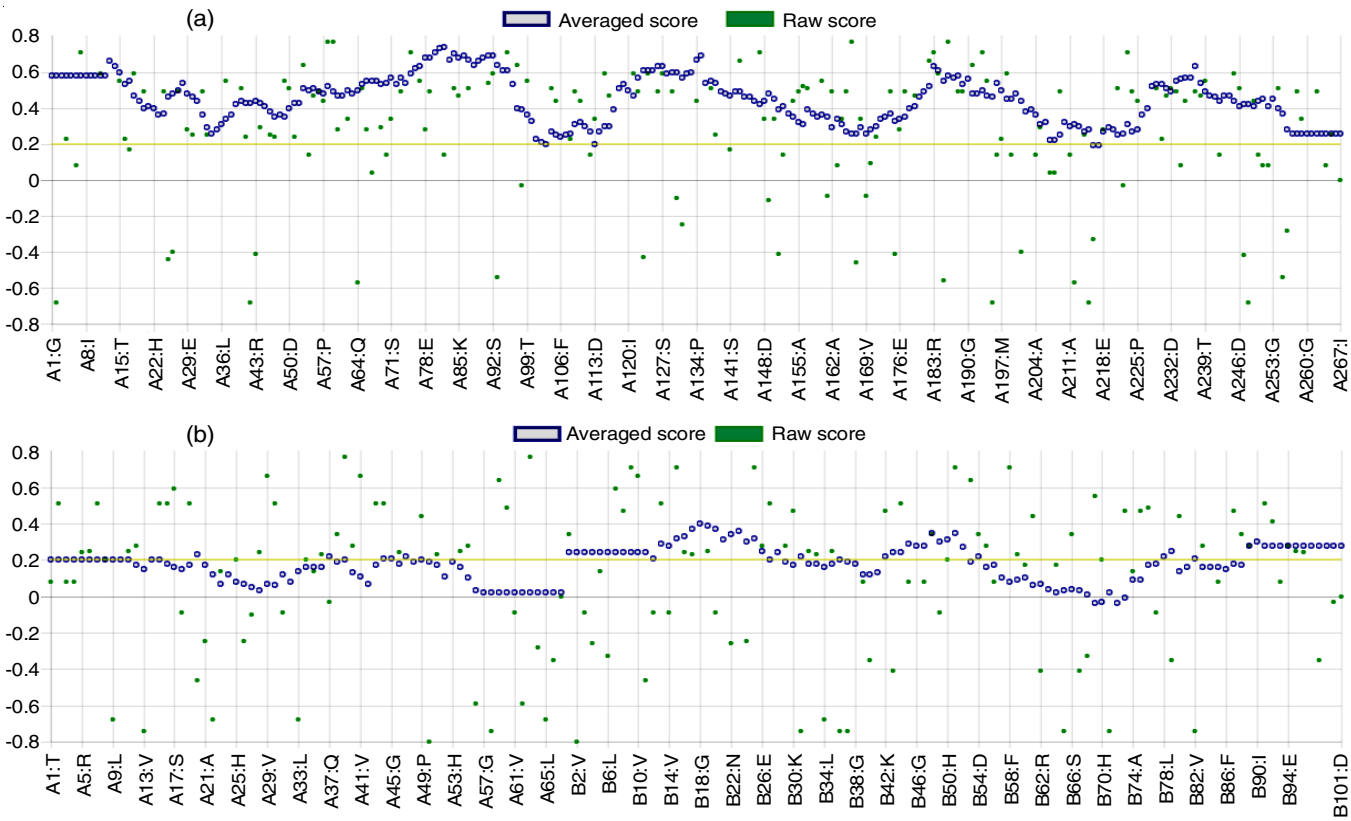

Fig. 3. Verify 3D results of (a) 2PR2 and (b) 1S14

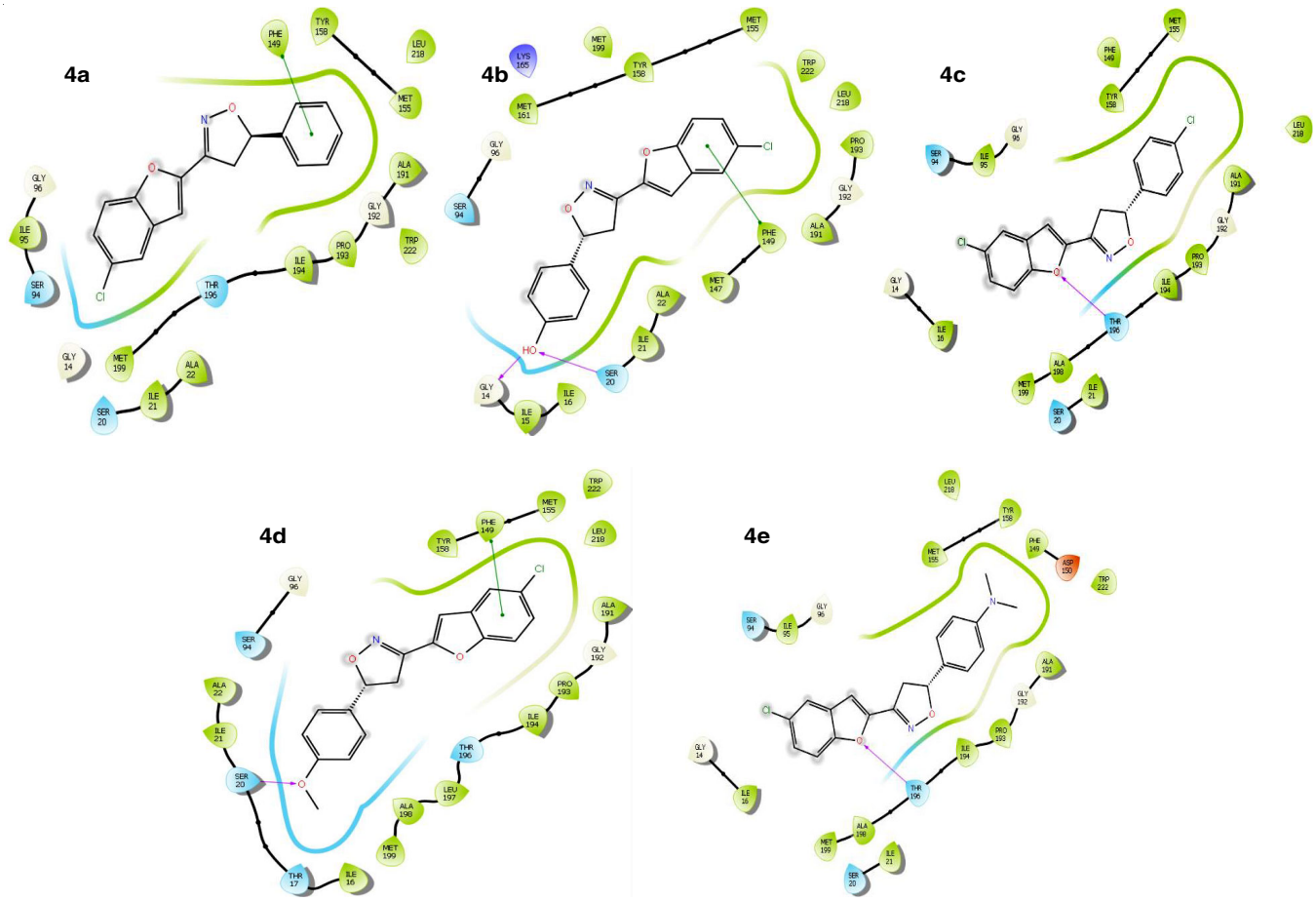

Fig. 4. Docking of synthesized compounds **4a-e** with 2PR2 protein

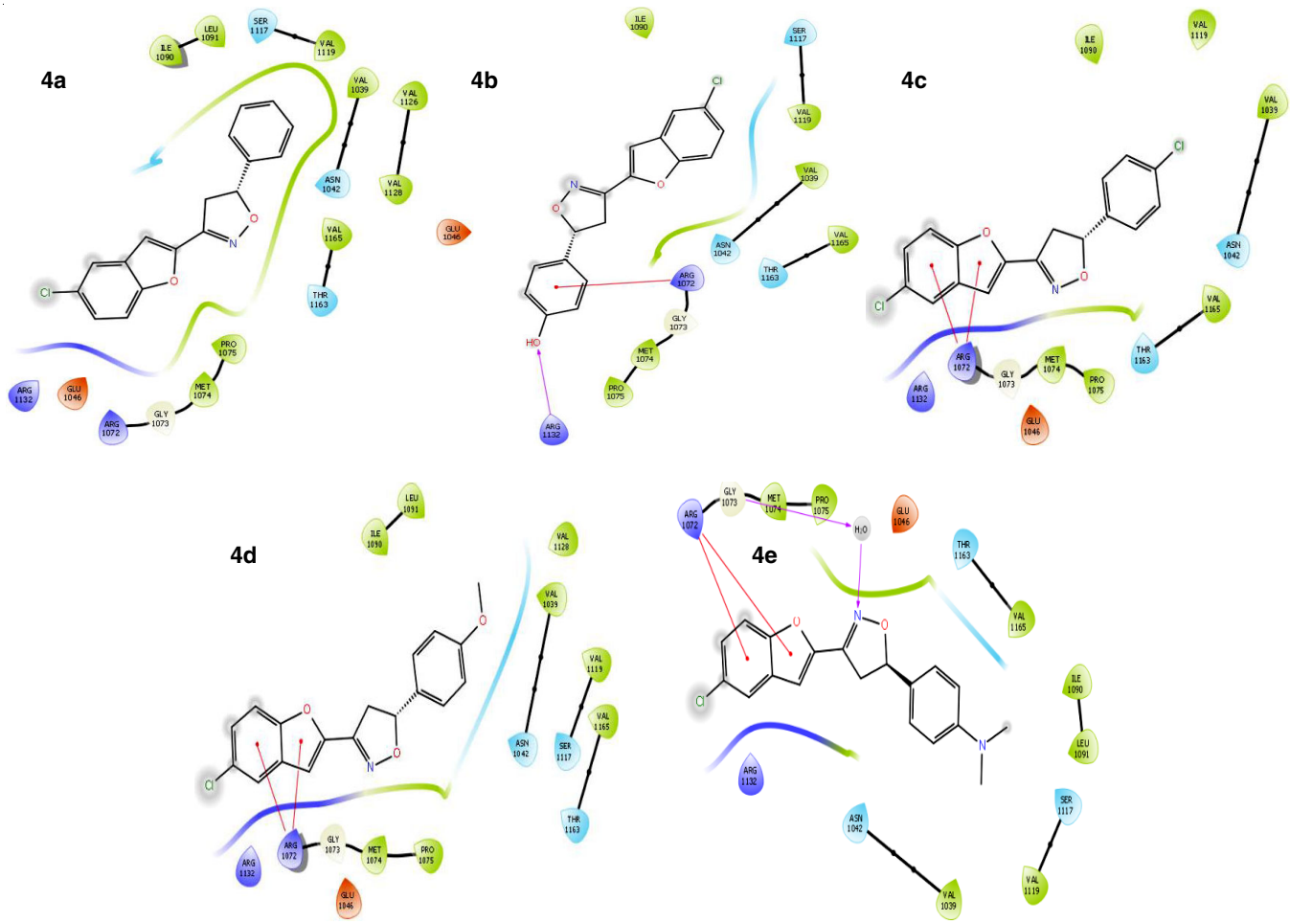

Fig. 5. Docking of synthesized compounds **4a-e** with 1S14 protein

TABLE-4
DOCKING SCORE AND MOLECULAR INTERACTION OF SYNTHESIZED COMPOUNDS WITH 2PR2 PROTEIN

Compound	Docking score	H-Bond interactions	Hydrophobic interactions
4a	-7.343	–	PHE 149
4b	-8.314	GLY 14, SER 20	PHE 149
4c	-6.599	THR 196	–
4d	-7.49	SER 20	PHE 149
4e	-7.507	THR 196	–
Isoniazid	-7.244	VAL 95, GLY 96	PHE 41

TABLE-5
DOCKING SCORE AND MOLECULAR INTERACTION OF SYNTHESIZED COMPOUNDS WITH 1S14 PROTEIN

Compound	Docking score	H-Bond interactions	Hydrophobic interactions
4a	-5.424	–	–
4b	-5.086	–	ARG 1072
4c	-5.322	–	ARG 1072
4d	-5.383	–	ARG 1072
4e	-5.995	GLY 1073	ARG 1072
Ciprofloxacin	-7.066	ASP 1069, GLY 1073	VAL 1118

It is indeed interesting to observe that synthesized compound **4e** shared one of the hydrogen bond interaction sites with the 1S14 protein model, which were comparable to the standard. In contrast, the remaining compounds **4a-d** did not exhibit any hydrogen bond interactions. However, they differed from the standard in terms of hydrophobic interaction sites. Notably, compound **4a** did not display either hydrogen bond or hydrophobic interactions; nevertheless, it surprisingly achieved the highest docking score when compared to the standard drug.

Antimicrobial activity: All the synthesized compounds **4a-e** underwent screening to evaluate their antitubercular and antibacterial activities. Regarding the antitubercular activity assessment, synthesized benzofuranyl-isoxazole hybrids (**4a-e**) were tested against *Mycobacterium tuberculosis* H37Rv in Middlebrook 7H9 broth media (MB 7H9 broth), with isoniazid serving as standard drug (Table-6). The results of the antitubercular activity screening indicated that compound **4c**, which features a *p*-chloro group and compound **4d**, containing *p*-methoxy group on the aromatic moiety at the 5th position of the isoxazole ring, exhibited activity at concentrations of 25, 50 and 100 µg/mL. However, the remaining three compounds **4a**, **4b** and **4e**, did not display significant activity in this context, except at a concentration of 100 µg/mL.

Furthermore, all the synthesized compounds underwent evaluation for their antibacterial activity using the agar cup-plate method, with ciprofloxacin serving as reference standard. Among these compounds (**4a-e**), notable antibacterial activity was observed at a dose level of 100 µg compared to the standard

TABLE-6
ANTITUBERCULAR ACTIVITY OF SYNTHESIZED COMPOUNDS (**4a-e**)

Compound	Minimum inhibitory concentration		
	25 µg/mL	50 µg/mL	100 µg/mL
4a	R	R	S
4b	R	R	S
4c	S	S	S
4d	S	S	S
4e	R	R	S
Isoniazid	S	S	S

drug (Fig. 6). Compounds **4c** and **4d** displayed the highest activity among all the tested bacterial strains. This heightened activity can be attributed to the presence of distinct electronically active groups, namely the *p*-chloro and *p*-methoxy groups located on the phenyl ring at the 5th position of the isoxazole.

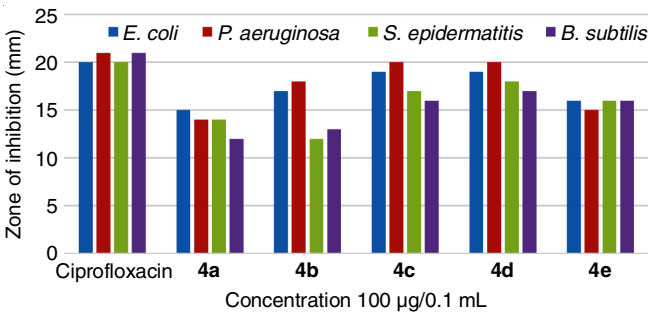

Fig. 6. Antibacterial activity of synthesized compounds **4a-e** (Gram-negative = *E. coli*, *P. aeruginosa*; Gram-positive = *S. epidermatitis*, *B. subtilis*)

Furthermore, all the compounds demonstrated significant antibacterial activity against a variety of bacterial strains. This can be attributed to the assortment of substituents situated at the *para*-position of the aryl rings, including hydroxyl and dimethylamino groups. Additionally, the presence of 5-chlorobenzofuran moiety had a beneficial impact on their antibacterial properties.

Conclusion

In conclusion, this study has explored the synthesis of benzofuran-isoxazole hybrids and their dual antimicrobial activities, with a specific focus on antitubercular and antibacterial potential. The compounds synthesized exhibit promise against tuberculosis and bacterial infections. *In silico* toxicity predictions provide insights into safety. Furthermore, the dual target docking studies conducted in this research have deepened the understanding of the potential mechanisms of action for these compounds against tuberculosis and bacteria. This molecular-level insight is crucial not only for elucidating their modes of action but also for addressing the challenging issue of antibiotic resistance in the context of bacterial infections.

ACKNOWLEDGEMENTS

The authors are thankful for the material support received from Sri Padmavathi School of Pharmacy, Tirupati, India.

CONFLICT OF INTEREST

The authors declare that there is no conflict of interests regarding the publication of this article.

REFERENCES

1. G. Bérubé, *Expert Opin. Drug Discov.*, **11**, 281 (2016); https://doi.org/10.1517/17460441.2016.1135125
2. S. Maddela, G.E. Mathew, D.G.T. Parambi, F. Aljoufi and B. Mathew, *Lett. Drug Des. Discov.*, **16**, 220 (2019); https://doi.org/10.2174/1570180815666180516102100
3. D.S. Reddy, M. Kongot and A. Kumar, *Tuberculosis*, **127**, 102050 (2021); https://doi.org/10.1016/j.tube.2020.102050
4. E. Kabir and M. Uzzaman, *Results Chem.*, **4**, 100606 (2022); https://doi.org/10.1016/j.rechem.2022.100606
5. H. Khanam and Shamsuzzaman, *Eur. J. Med. Chem.*, **97**, 483 (2015); https://doi.org/10.1016/j.ejmech.2014.11.039
6. B. Bhukya, A. Shukla, V. Chaturvedi, P. Trivedi, S. Kumar, F. Khan, A.S. Negi and S.K. Srivastava, *Bioorg. Chem.*, **99**, 103784 (2020); https://doi.org/10.1016/j.bioorg.2020.103784
7. Z. Xu, S. Zhao, Z. Lv, L. Feng, Y. Wang, F. Zhang, L. Bai and J. Deng, *Eur. J. Med. Chem.*, **162**, 266 (2019); https://doi.org/10.1016/j.ejmech.2018.11.025
8. A.A. Abbas and K.M. Dawood, *Expert Opin. Drug Discov.*, **17**, 1357 (2022); https://doi.org/10.1080/17460441.2023.2157400
9. C. Mahecha-Mahecha, P. Borrego-Muñoz, L.M. Pombo and D. Gamba-Sánchez, *RSC Adv.*, **13**, 25296 (2023); https://doi.org/10.1039/D3RA04737G
10. Y. Chen, R. Chen, R. Yuan, L. Huo, H. Gao, Y. Zhuo, X. Chen, C. Zhang and S. Yang, *Int. J. Mol. Sci.*, **24**, 3575 (2023); https://doi.org/10.3390/ijms24043575
11. A.A. Abbas and K.M. Dawood, *RSC Adv.*, **13**, 11096 (2023); https://doi.org/10.1039/D3RA01383A
12. K.M. Dawood, *Expert Opin. Ther. Pat.*, **29**, 841 (2019); https://doi.org/10.1080/13543776.2019.1673727
13. N.J. Siddiqui and M. Idrees, *Der Pharma Chem.*, **6**, 406 (2014).
14. Y. Kanzouai, M. Laghmari, I. Yamari, R. Bouzammit, L. Bahsis, T. Benali, S. Chtita, M. Bakhouch, M. Akhazzane, M. El-Kouali, K. Hammani and G. Al Houari, *J. Biomol. Struct. Dyn.*, 1 (2023); https://doi.org/10.1080/07391102.2023.2266022
15. A. Nagaraju, S.K. Nukala, N.S. Thirukovela and R. Manchal, *Chem. Biol. Lett.*, **10**, 542 (2023).
16. G.C. Arya, K. Kaur and V. Jaitak, *Eur. J. Med. Chem.*, **221**, 113511 (2021); https://doi.org/10.1016/j.ejmech.2021.113511
17. F. Vafadarnejad, M. Saeedi, M. Mahdavi, A. Rafinejad, E. Karimpour-Razkenari, B. Sameem, M. Khanavi and T. Akbarzadeh, *Lett. Drug Des. Discov.*, **14**, 712 (2017); https://doi.org/10.2174/1570180813666161018124726
18. A. Saleem, U. Farooq, S.M. Bukhari, S. Khan, A. Zaidi, T.A. Wani, A.J. Shaikh, R. Sarwar, S. Mahmud, M. Israr, F.A. Khan and S.A. Shahzad, *ACS Omega*, **7**, 30359 (2022); https://doi.org/10.1021/acsomega.2c03600
19. K. Manna, Y.K. Agarwal and K.K. Srinivasan, *Indian J. Heterocycl. Chem.*, **18**, 87 (2008).
20. N. Umapathi, B. Shankar, M. Raghavender, T. Vishnu and P. Jalapathi, *Russ. J. Gen. Chem.*, **91**, S112 (2021); https://doi.org/10.1134/S1070363222020256
21. V.K. Kumar, V. Puli, K.R.S. Prasad and G. Sridhar, *Chem. Data Coll.*, **36**, 100787 (2021); https://doi.org/10.1016/j.cdc.2021.100787
22. TB/COVID-19 Global Study Group, *Eur. Respir. J.*, **59**, 2102538 (2022); https://doi.org/10.1183/13993003.02538-2021
23. T. Shah, Z. Shah, N. Yasmeen, Z. Baloch and X. Xia, *Front. Immunol.*, **13**, 909011 (2022); https://doi.org/10.3389/fimmu.2022.909011

24. P. Daneshvar, B. Hajikhani, F. Sameni, N. Noorisepehr, N. Bostanshirin, F. Zare, S. Yazdani, M. Goudarzi, S. Sayyari and M. Dadashi, *Heliyon*, **9**, e13637 (2023); https://doi.org/10.1016/j.heliyon.2023.e13637
25. R.K. Kumarachari, M. Guruvareddy, M. Phebe, P.L. Reddy, M.S. Nithin, D. Lakshmipathi and M. Manasa, *Asian J. Chem.*, **35**, 617 (2023); https://doi.org/10.14233/ajchem.2023.27482
26. A.V. Sadybekov and V. Katritch, *Nature*, **616**, 673 (2023); https://doi.org/10.1038/s41586-023-05905-z
27. D.A. Filimonov, A.A. Lagunin, T.A. Gloriozova, D.S. Druzhilovskii, A.V. Rudik, P.V. Pogodin and V.V. Poroikov, *Chem. Heterocycl. Compd.*, **50**, 444 (2014); https://doi.org/10.1007/s10593-014-1496-1
28. A. Ayar, M. Aksahin, S. Mesci, B. Yazgan, M. Gül and T. Yýldýrým, *Curr. Computeraided Drug Des.*, **18**, 52 (2022); https://doi.org/10.2174/1573409917666210223105722
29. T. Sander, Actelion's Property Explorer, Allschwil, Switzerland: Actelion's Pharmaceuticals Ltd. (2001).
30. A. Daina, O. Michielin and V. Zoete, *Sci. Rep.*, **7**, 42717 (2017); https://doi.org/10.1038/srep42717
31. R.A. Friesner, R.B. Murphy, M.P. Repasky, L.L. Frye, J.R. Greenwood, T.A. Halgren, P.C. Sanschagrin and D.T. Mainz, *J. Med. Chem.*, **49**, 6177 (2006); https://doi.org/10.1021/jm051256o
32. D. Eisenberg, R. Luthy and J.U. Bowie, *Methods Enzymol.*, **277**, 396 (1997); https://doi.org/10.1016/S0076-6879(97)77022-8
33. C. Colovos and T.O. Yeates, *Protein Sci.*, **2**, 1511 (1993); https://doi.org/10.1002/pro.5560020916
34. S. Analysis and V. Server (2011); Available from: http://nihserver.mbi.ucla.edu/SAVES/
35. S.C. Lovell, I.W. Davis, W.B. Arendall 3rd, P.I. de Bakker, J.M. Word, M.G. Prisant, J.S. Richardson and D.C. Richardson, *Proteins*, **50**, 437 (2003); https://doi.org/10.1002/prot.10286
36. Cambridge Soft Corporation, a subsidiary of PerkinElmer, Inc. (2014). Chem DrawUltra version 8.0.3 for Windows. Available from: www.cambridgesoft.com.
37. https://sourceforge.net/projects/openbabel/files/openbabel/2.4.0/; License: GNU GPL v2.
38. N.M. O'Boyle, M. Banck, C.A. James, C. Morley, T. Vandermeersch and G.R. Hutchison, *J. Cheminform.*, **3**, 33 (2011); https://doi.org/10.1186/1758-2946-3-33
39. E. Harder, W. Damm, J. Maple, C. Wu, M. Reboul, J.Y. Xiang, L. Wang, D. Lupyan, M.K. Dahlgren, J.L. Knight, J.W. Kaus, D.S. Cerutti, G. Krilov, W.L. Jorgensen, R. Abel and R.A. Friesner, *J. Chem. Theory Comput.*, **12**, 281 (2016); https://doi.org/10.1021/acs.jctc.5b00864
40. S.G. Franzblau, R.S. Witzig, J.C. McLaughlin, P. Torres, G. Madico, A. Hernandez, M.T. Degnan, M.B. Cook, V.K. Quenzer, R.M. Ferguson and R.H. Gilman, *J. Clin. Microbiol.*, **36**, 362 (1998); https://doi.org/10.1128/JCM.36.2.362-366.1998
41. B. Aneja, M. Azam, A. Perwez, R. Maguire, U. Yadava, K. Kavanagh, S. Alam, C.G. Daniliuc, M.M.A. Rizvi, Q.M.R. Haq and M. Abid, *ACS Omega*, **3**, 6912 (2018); https://doi.org/10.1021/acsomega.8b00582
42. CLSI, M100 Performance Standards for Antimicrobial Susceptibility Testing, 29th ed. CLSI; Wayne, PA, USA (2019).